Volume 14 | Number 23 | 21 June 2018 | Pages 4651–4882

Soft Matter

rsc.li/soft-matter-journal

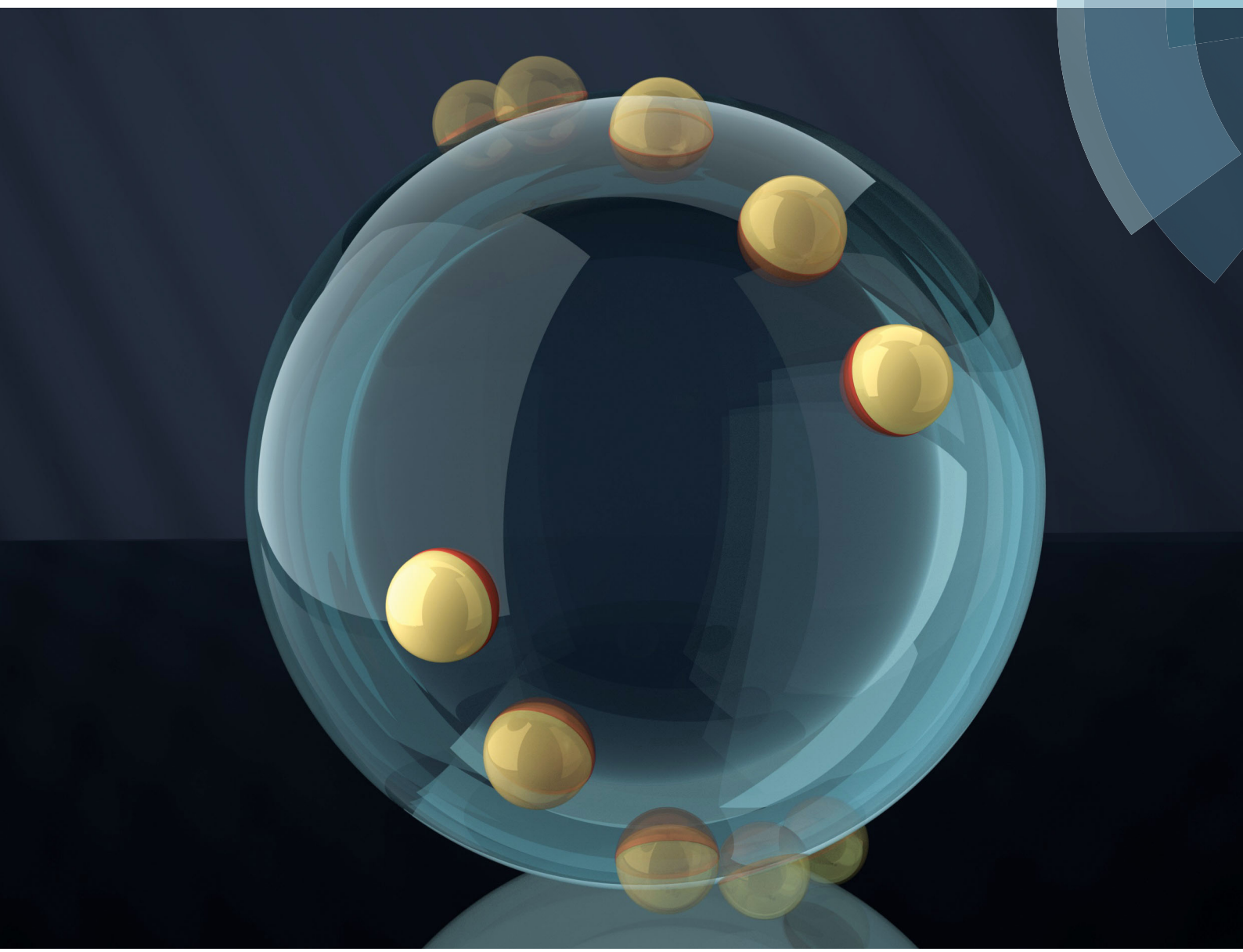

ISSN 1744-6848

ROYAL SOCIETY OF CHEMISTRY

COMMUNICATION

Kyle J. M. Bishop *et al.*

Magneto-capillary dynamics of amphiphilic Janus particles at curved liquid interfaces

Soft Matter

COMMUNICATION

View Article Online
View Journal | View Issue

Cite this: *Soft Matter*, 2018, **14**, 4661

Received 13th March 2018,
Accepted 2nd May 2018

DOI: 10.1039/c8sm00518d

rsc.li/soft-matter-journal

Magneto-capillary dynamics of amphiphilic Janus particles at curved liquid interfaces†

Wenjie Fei,[a] Michelle M. Driscoll,[b] Paul M. Chaikin[b] and Kyle J. M. Bishop *[a]

A homogeneous magnetic field can exert no net force on a colloidal particle. However, by coupling the particle's orientation to its position on a curved interface, even static homogeneous fields can be used to drive rapid particle motions. Here, we demonstrate this effect using magnetic Janus particles with amphiphilic surface chemistry adsorbed at the spherical interface of a water drop in decane. Application of a static homogeneous field drives particle motion to the drop equator where the particle's magnetic moment can align parallel to the field. As explained quantitatively by a simple model, the effective magnetic force on the particle scales linearly with the curvature of the interface. For particles adsorbed on small droplets such as those found in emulsions, these magneto-capillary forces can far exceed those due to magnetic field gradients in both magnitude and range. This mechanism may be useful in creating highly responsive emulsions and foams stabilized by magnetic particles.

Introduction

The actuation of microscale particles by magnetic fields provides a basis for the development of responsive materials,[1–3] active particle assemblies,[4,5] and colloidal robots[6,7] with increasing functionality. In contrast to electric and optical fields, magnetic fields are not screened or scattered by common materials and can therefore act remotely, instantaneously, and specifically on magnetic particles introduced for a desired purpose. Such particles are characterized by a magnetic dipole moment $\boldsymbol{m}$, which determines their response to an applied field $\boldsymbol{B}$. Notably, a homogeneous field induces no force on a magnetic particle but rather a torque, $\boldsymbol{L} = \boldsymbol{m} \times \boldsymbol{B}$, that acts to align the moment parallel to the field. The generation of magnetic forces requires spatial gradients in the field, $\boldsymbol{F} = \boldsymbol{m}\cdot\nabla\boldsymbol{B}$, which allow for three-dimensional positioning of magnetic particles.[8] In practice, however, this approach is limited by the complexity of the required fields and by the magnitude of the forces generated. As a result, other strategies for positioning or propelling magnetic particles have been explored using time-varying homogeneous fields.[9,10] In particular, rotating fields induce steady torques that couple to particle translation in viscous fluids through the design of particle shape[11,12] or the proximity of fluid boundaries.[5,13] The use of hydrodynamics to couple magnetic torque to particle translation suggests that other physics might be used to enable new forms of magnetic positioning in static homogeneous fields.

One approach to coupling the orientation and position of a colloidal particle is to confine its motion along a curved interface. Particles of asymmetric shape[14] or surface chemistry[15] are known to adsorb spontaneously at fluid–fluid interfaces in a preferred orientation that minimizes the interfacial energy. Particle motion along a curved interface is therefore accompanied by particle rotation as to maintain this orientation. By exploiting the coupling between particle position and orientation, it should be possible to translate applied torques into particle motions across curved interfaces. In particular, magnetic particles could be driven to move by application of static homogeneous fields.[16] This idea was recently investigated using numerical simulations;[17] however, it has yet to be demonstrated in experimental practice. The use of homogeneous fields to redistribute magnetic particles at liquid interfaces has important implications for the design of field-responsive emulsions[1] and foams.[2,3]

Here, we investigate the motion of magnetic Janus particles (MJPs)[18–22] along curved decane–water interfaces in response to static homogeneous fields. Owing to their amphiphilic surface chemistry, the MJPs adsorb onto spherical water drops with their magnetic nickel hemisphere positioned in the aqueous phase. Application of the magnetic field causes the particles to move along the drop surface to align their magnetic moments parallel to the field. These motions are captured quantitatively by a simple model that accounts for the magnetic torque on the particle and the constraints imposed by the interface. We show how the particle velocity increases with increasing field

[a] *Department of Chemical Engineering, Columbia University, New York, NY, USA. E-mail: kyle.bishop@columbia.edu*

[b] *Department of Physics, New York University, New York, NY, USA*

† Electronic supplementary information (ESI) available: Orientation of MJPs at planar interfaces; magnetic rolling experiments; characterization of the homogeneous magnetic field; model of particle dynamics with gravity; detailed description of data analysis. See DOI: 10.1039/c8sm00518d

strength and with decreasing drop radius R. Notably, the effective magnetic force, $F \sim mB/R$, experienced by particles adsorbed on small drops can be many orders of magnitude larger than those due to field gradients. This result suggests that asymmetric magnetic particles may be useful for creating highly responsive emulsions and foams with tunable morphology and stability.

Experiment

Our experiments were based on magnetic Janus particles (MJPs) with amphiphilic surface chemistry (Fig. 1a, inset). To prepare the particles, we first deposited successive layers of metal – 5 nm Ti adhesive layer, 25 nm Ni magnetic layer, and 20 Au functionalization layer – onto monolayers of 4 μm fluorescent sulfonated polystyrene (PS) particles by e-beam evaporation.[20] The gold hemispheres of the MJPs were rendered hydrophilic by chemical functionalization with 3-mercaptopropionic acid (MPA) ligands.[23] Such particles were observed to adsorb at the decane–water interface with their MPA-functionalized hemispheres directed toward the aqueous phase in agreement with previous reports (Fig. S1, ESI†).[23] Additionally, the nickel layer gave the particles a permanent magnetic moment $m \approx 3 \times 10^{-14}$ A m^2 directed parallel to the Janus equator.[4,24] The particles' magnetic properties were determined from measurements of particle translation along a solid substrate ("rolling") in a rotating magnetic field as a function of the applied frequency (Fig. S2, ESI†).[5]

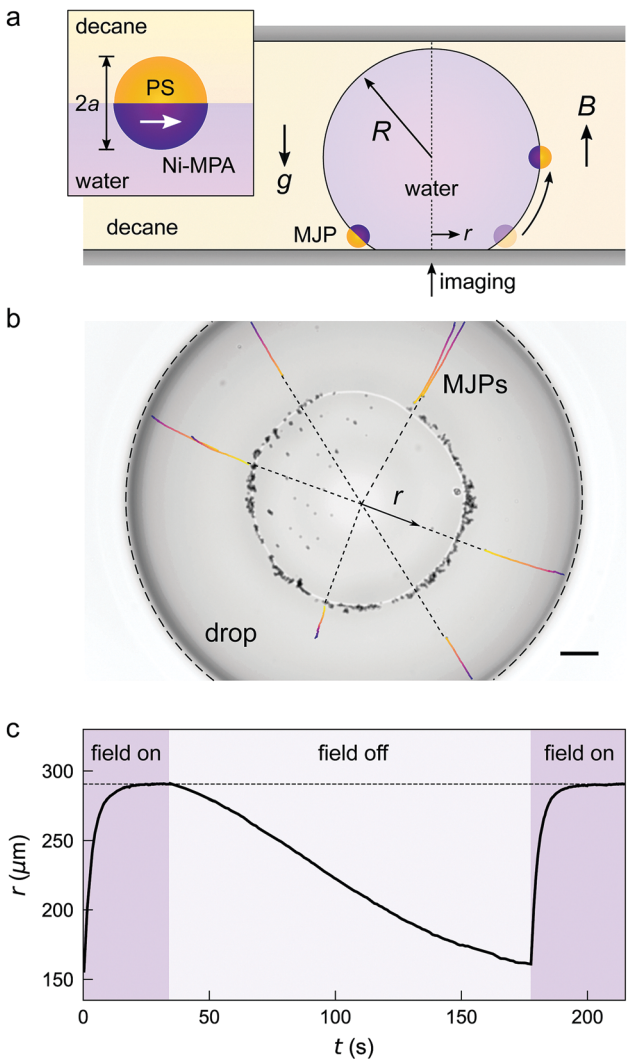

Fig. 1 (a) Schematic illustration of a magnetic Janus particle (MJP) moving on the curved interface of a water drop in decane due to a homogeneous magnetic field $\boldsymbol{B}$. The inset shows the preferred orientation of the MJP at the interface and its magnetic moment (white arrow). (b) Optical micrograph of the water drop showing the radial trajectories of six different MJPs; scale bar is 100 μm. (c) Projected radial position of an MJP as a function of time for successive applications of the magnetic field. Here, the field strength is B = 15 mT, and the drop radius is R = 291 μm.

MJPs were spread onto the curved interface of a water drop in decane supported between two hydrophobic glass slides (Fig. 1a). A drop of water (~0.5 μL) was first deposited onto a cover slip treated with a hydrophobic silane. Amphiphilic MJPs suspended in a mixture of water and isopropyl alcohol (7 : 3 ratio) were spread onto the interface using a micropipette. The cover slip was then incorporated as the base of a glass chamber, into which decane was flowed.[25] The chamber was sealed with UV-curable epoxy (NOA 68) and positioned on the stage of an inverted microscope for imaging. The particles settled under gravity to the three-phase contact line at the bottom of the drop (Fig. 1b).

Application of a magnetic field $\boldsymbol{B}$ antiparallel to the gravity direction caused the particles to migrate to the drop equator along radial trajectories (Fig. 1b). Two electromagnet coils positioned above and below the drop created a spatially uniform field with variations of less than 0.5% within the 0.4 cm^3 region of interest (Fig. S3, ESI†). Upon application of the field, some particles moved radially outward from the axis of symmetry along the interface of the drop. Others remained pinned at the three-phase contact line and did not move (Fig. 1b), perhaps due to attractive surface forces with the hydrophobic substrate. Particle motions were captured by fluorescent video microscopy, during which the focal plane was manually adjusted to keep the particle in focus as it moved to the drop equator. Particle trajectories projected onto the imaging plane were reconstructed from the videos using standard particle tracking algorithms (Trackpy v0.3.2). When the field was switched off, the mobile particles slowly settled back toward the three-phase contact line. By cycling the magnetic field on and off, we captured multiple trajectories of a single particle moving on the interface of single drop (Fig. 1c).

Results and discussion

The experimental observations are explained by a simple model that accounts for the magnetic torque on the particle and the constraints imposed by its amphiphilic surface chemistry. The magnetic energy of the system is minimal when the particle's magnetic moment $\boldsymbol{m}$ is aligned parallel with the applied field $\boldsymbol{B}$. Similarly, the interfacial energy of the system is minimal when the symmetry axis of the amphiphilic MJP is aligned perpendicular to the interface. For the particles described here, both

conditions are satisfied only when the particle is located at the drop equator. At other locations, magnetic and interfacial torques compete with one another to drive rotational and translational particle motions.

The characteristic scale of the magnetic torque mB is much smaller than that of the interfacial torque γa^2 where γ is the interfacial tension; here, $mB/\gamma a^2 \sim 0.002 \ll 1$. Consequently, the applied field does little to change the preferred orientation of the particle axis relative to the interface;[26] such rotations are effectively prohibited by the particle's amphiphilic surface chemistry. By contrast, the particle is free to rotate about its symmetry axis and to translate across the surface of the drop without changing the interfacial energy. Importantly, the constraints imposed by the interface allow one to translate magnetic torques applied to the particle into translational motions along the drop surface.

The position and orientation of an MJP adsorbed at the interface of a spherical drop can be specified by three angles: the polar angle θ, the azimuthal angle φ, and the orientation angle β that describes the direction of the particle's magnetic moment in the plane of the interface (Fig. 2). The angle α between the particle's magnetic moment and the unit vector normal to the interface is assumed to be constant (Fig. 2); $\alpha = \pi/2$ in our experiments. In a uniform magnetic field $\boldsymbol{B} = B\boldsymbol{e}_z$, the magnetic energy of a single ferromagnetic particle is $U = -\boldsymbol{m}\cdot\boldsymbol{B}$. By differentiating this expression with respect to each coordinate, we obtain the generalized forces that act to move and rotate the particle on the drop interface. At low Reynolds numbers, these forces are balanced by the viscous drag, resulting in the following overdamped dynamics

$$\dot{\theta} = -\frac{1}{\lambda_t R^2}\frac{\partial U}{\partial \theta} = \frac{mB}{\lambda_t R^2}(\sin\alpha\cos\beta\cos\theta + \cos\alpha\sin\theta), \qquad (1)$$

$$\dot{\beta} = -\frac{1}{\lambda_r}\frac{\partial U}{\partial \beta} = -\frac{mB}{\lambda_r}\sin\alpha\sin\beta\sin\theta, \qquad (2)$$

where $\lambda_t \approx 6\pi\eta a$ and $\lambda_r \approx 8\pi\eta a^3$ are drag coefficients for translation and rotation, respectively, and $\eta = 9.1 \times 10^{-4}$ Pa s is an effective fluid viscosity at the interface. For spherical drops, there is no particle motion in the azimuthal direction since $\partial U/\partial\varphi = 0$.

These dynamics can be solved analytically when the particle is much smaller than the drop ($a \ll R$). Under these conditions, the orientation angle β relaxes quickly to a stable value of $\beta = \pi$, and the particle moves slowly to its stable position. Integrating eqn (1) with $\alpha = \pi/2$ and $\beta = \pi$, we obtain the following expression for the projected radial position measured in experiment

$$r(t) = R\sin\left\{2\tan^{-1}\left[\tanh\left(\frac{1}{2}k_m t + C\right)\right]\right\}. \qquad (3)$$

Here, $C > 0$ is a constant that determines the position of the particle at $t = 0$, and $k_m \equiv mB/\lambda_t R^2$ is the characteristic rate for magnetic particle actuation. Physically, the particle moves to the equator of the drop ($r \to R$) to align its magnetic moment with the applied field. This model can be generalized to include the effects of gravity as detailed in the ESI.†

The model predicts that the rate of magnetic actuation should increase with decreasing drop size as $k_m \propto R^{-2}$. To evaluate this prediction, we measured the field-induced particle trajectories on droplets of different sizes (Fig. 3a). For each drop, we tracked the motion of a single particle during several cycles of magnetic actuation and sedimentation under gravity. For each particle, we used Bayesian inference[27] with Markov

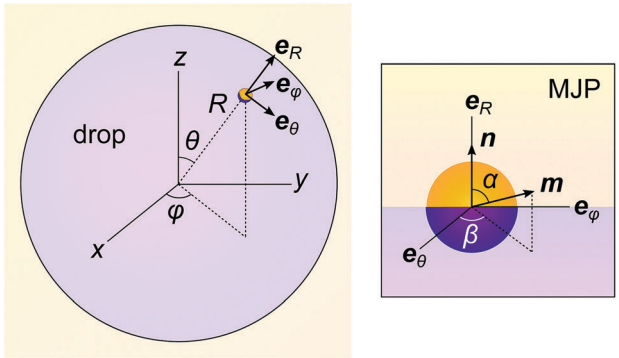

Fig. 2 The position and orientation of an amphiphilic Janus particle on a spherical drop can be described by the angles θ, φ, and β. The angle α between the particle's permanent magnetic moment $\boldsymbol{m}$ and the unit normal vector $\boldsymbol{n}$ is held constant by interfacial forces.

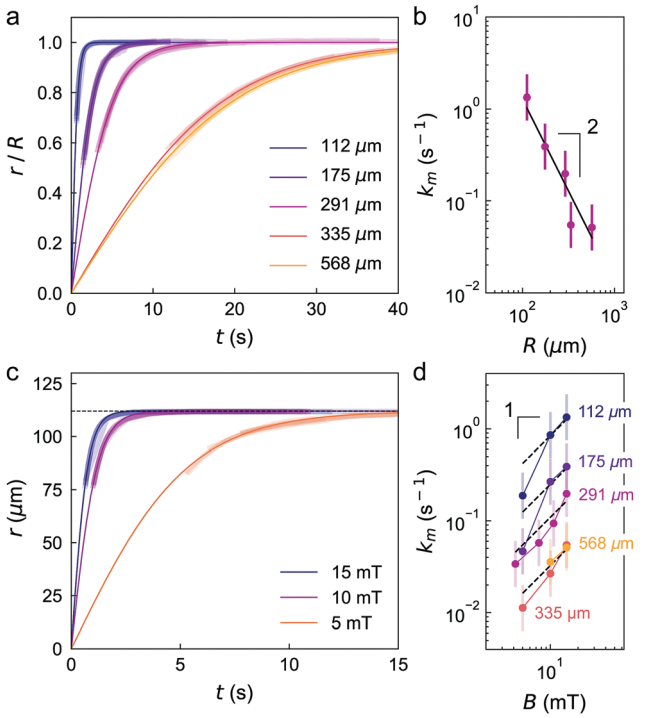

Fig. 3 (a) Projected radial trajectories of MJPs on drops of different radii for B = 15 mT. For each drop, the wide curves show multiple tracks from a single particle superimposed over the model prediction (thin curve). (b) Rate parameter *vs.* drop radius inferred from the data in (a). (c) Projected radial trajectories of a single MJP moving on a drop of radius R = 112 μm at different field strengths. (d) Fitted rate parameter *vs.* field strength for different drop radii. Error bars denote one standard deviation above and below the mean.

chain Monte Carlo (MCMC) sampling[28] to estimate the rate parameter k_m from the reconstructed trajectories (see ESI† for details). Fig. 3b shows the inferred rate parameter as a function of the drop radius for a constant field strength of $B = 15$ mT.

The experimental results agree with the model predictions of eqn (3) when accounting for the observed variability in the motions of different particles. For each particle, the root-mean-square (rms) error in the rate parameter was small (*ca.* 0.6% of the mean), indicating good reproducibility during successive applications of the field. In the rare cases when multiple mobile particles were present on the same drop, we analyzed each particle separately to assess the variability in the rate parameter from one particle to the next. The motions of different particles subject to identical conditions varied by *ca.* 60%, perhaps due to differences in their magnetic moments, their orientation at the interface, or their resistance to motion.[29] The error bars in Fig. 3 represent this larger variability in the motions of different particles. Using the data in Fig. 3b, we infer the average magnetic moment of the particles to be $m = 2.9 \times 10^{-14}$ A m^2, which agrees well with independent estimates from our magnetic characterization (Fig. S2, ESI†).

The model also predicts that the rate parameter k_m should increase linearly with the magnitude of the applied field. To test this prediction, we varied the applied field over the experimentally accessible range of $B = 4$–15 mT. Larger fields were inaccessible due to significant Joule heating of the electromagnet coils; smaller fields led to weak magnetic forces that struggled to compete with those due to gravity. Fig. 3b shows the projected radial trajectories for a single MJP adsorbed on a drop of radius $R = 112$ μm for three different field strengths. From these data, we inferred the rate parameter k_m for each field strength assuming the validity of eqn (3). The inferred rate increased monotonically with increasing field strength but deviated from the expected linear dependence – particularly at weak fields (Fig. 3d).

The failure of the model at weak fields is likely caused by other forces due to gravity, light-induced Marangoni stresses, or gradients in the drop curvature. The predicted dynamics of MJPs moving under the influence of both magnetic and gravitational fields is derived in the ESI.† This augmented model is characterized by an additional dimensionless parameter, $G \equiv MgR/mB$, which measures the relative importance of gravitational and magnetic forces (here, M is the bouyant mass of the particle, and g is the acceleration due to gravity). At low fields, this parameter is $G = 0.2$, and the effects of gravity cannot be neglected. However, even when accounting for gravitational forces, the inferred rate parameter k_m was still considerable smaller than that predicted by theory (Fig. S8, ESI†).

In addition to gravity, spatial variations in the interfacial curvature and tension give rise to other forces that may alter magneto-capillary particle motions. MJPs adsorbed at liquid interfaces are known to induce capillary disturbances that interact with the curvature field imposed by the interface.[23,30,31] Such capillary forces are absent for particles adsorbed at spherical interfaces, which have zero deviatoric curvature (*i.e.*, equal principal curvatures, $c_1 = c_2 = 1/R$). However, it is possible that the drops used here deviate slightly from their ideal spherical shape (*e.g.*, due to gravity or pinning of the three-phase contact line) resulting in nonzero capillary forces. A more likely explanation for the anomalous behavior at low field strengths is motion due to Marangoni stresses caused by light-induced heating of the particles. Particles at liquid interfaces are known to move *via* self-generated surface tension gradients when heated by irradiation with visible light.[32] Under bright illumination (5.4 mW mm^{-2}), the field-induced motions of our MJPs were observed to deviate significantly from those at low illumination (0.15 mW mm^{-2}) detailed above. At low field strengths, magneto-capillary forces may compete with light-powered Marangoni propulsion in directing the motion of MJPs along curved interfaces (Fig. S5, ESI†).

Conclusions

The constraints imposed by a liquid interface on the motions of magnetic Janus particles enables uniform magnetic fields to induce strong magnetic forces of order $F_m \sim mB/R$. For particles adsorbed on small droplets such as those found in emulsions, these magneto-capillary forces can far exceed those due to magnetic field gradients in both magnitude and range. This mechanism may therefore be useful in controlling the stability, drop size, and morphology of emulsions and foams stabilized by magnetic particles.[1,2,33] For example, the application of a uniform magnetic field could drive the redistribution of MJPs on the surface of emulsion drops, thereby altering their stability to coalescence along specified directions (*e.g.*, at the drop poles). In this context, further work is required to understand the impact of interfacial rheology on field-induced particle motions at complex fluid interfaces.[34,35] We emphasize that the magneto-capillary forces described here are not limited to magnetic Janus particles, which provide a convenient model system. Similar behaviors are also expected for other anisotropic particles that adsorb at liquid interfaces in a preferred orientation[14] and respond to external magnetic fields (*e.g.*, hematite ellipsoids[36]). Beyond the simple dynamics described here, more complex particle motions are possible using spatially uniform fields with time-varying magnitude and direction.

Conflicts of interest

There are no conflicts to declare.

Acknowledgements

This work was supported as part of the Center for Bio-Inspired Energy Science, an Energy Frontier Research Center funded by the U.S. Department of Energy, Office of Science, Basic Energy Sciences under Award DE-SC0000989. M. M. D. was supported by the Gordon and Betty Moore Foundation through Grant GBMF3849.

References

1 S. Melle, M. Lask and G. G. Fuller, *Langmuir*, 2005, **21**, 2158–2162.
2 S. Lam, E. Blanco, S. K. Smoukov, K. P. Velikov and O. D. Velev, *J. Am. Chem. Soc.*, 2011, **133**, 13856–13859.

3 E. Blanco, S. Lam, S. K. Smoukov, K. P. Velikov, S. A. Khan and O. D. Velev, *Langmuir*, 2013, **29**, 10019–10027.
4 J. Yan, S. C. Bae and S. Granick, *Soft Matter*, 2015, **11**, 147–153.
5 M. Driscoll, B. Delmotte, M. Youssef, S. Sacanna, A. Donev and P. Chaikin, *Nat. Phys.*, 2017, **13**, 375–380.
6 B. J. Nelson, I. K. Kaliakatsos and J. J. Abbott, *Annu. Rev. Biomed. Eng.*, 2010, **12**, 55–85.
7 K. Han, C. W. Shields and O. D. Velev, *Adv. Funct. Mater.*, 2018, 1705953.
8 M. P. Kummer, J. J. Abbott, B. E. Kratochvil, R. Borer, A. Sengul and B. J. Nelson, *IEEE Trans. Robot.*, 2010, **26**, 1006–1017.
9 R. Dreyfus, J. Baudry, M. L. Roper, M. Fermigier, H. A. Stone and J. Bibette, *Nature*, 2005, **437**, 862–865.
10 K. Han, C. W. Shields, N. M. Diwakar, B. Bharti, G. P. López and O. D. Velev, *Sci. Adv.*, 2017, **3**, e1701108.
11 L. Zhang, J. J. Abbott, L. Dong, B. E. Kratochvil, D. Bell and B. J. Nelson, *Appl. Phys. Lett.*, 2009, **94**, 064107.
12 A. Ghost and P. Fischer, *Nano Lett.*, 2009, **9**, 2243–2245.
13 F. Martinez-Pedrero, A. Ortiz-Ambriz, I. Pagonabarraga and P. Tierno, *Phys. Rev. Lett.*, 2015, **115**, 138301.
14 J. C. Loudet, A. M. Alsayed, J. Zhang and A. G. Yodh, *Phys. Rev. Lett.*, 2005, **94**, 018301.
15 A. Kumar, B. J. Park, F. Tu and D. Lee, *Soft Matter*, 2013, **9**, 6604–6617.
16 W. Fei, Y. Gu and K. J. Bishop, *Curr. Opin. Colloid Interface Sci.*, 2017, **32**, 57–68.
17 Q. Xie, G. B. Davies and J. Harting, *ACS Nano*, 2017, **11**, 11232–11239.
18 R. M. Erb, N. J. Jenness, R. L. Clark and B. B. Yellen, *Adv. Mater.*, 2009, **21**, 4825–4829.
19 S. K. Smoukov, S. Gangwal, M. Marquez and O. D. Velev, *Soft Matter*, 2009, **5**, 1285–1292.
20 I. Sinn, P. Kinnunen, S. N. Pei, R. Clarke, B. H. McNaughton and R. Kopelman, *Appl. Phys. Lett.*, 2011, **98**, 024101.
21 B. Ren, A. Ruditskiy, J. H. Song and I. Kretzschmar, *Langmuir*, 2012, **28**, 1149–1156.
22 J. Yan, M. Bloom, S. C. Bae, E. Luijten and S. Granick, *Nature*, 2012, **491**, 578–581.
23 B. J. Park, T. Brugarolas and D. Lee, *Soft Matter*, 2011, **7**, 6413.
24 K. Lee, Y. Yi and Y. Yu, *Angew. Chem., Int. Ed.*, 2016, **55**, 7384–7387.
25 C. P. Kelleher, R. E. Guerra, A. D. Hollingsworth and P. M. Chaikin, *Phys. Rev. E: Stat., Nonlinear, Soft Matter Phys.*, 2017, **95**, 022602.
26 Q. Xie, G. Davies, F. Günther and J. Harting, *Soft Matter*, 2015, **11**, 3581–3588.
27 D. S. Sivia and J. Skilling, *Data Analysis: A Bayesian Tutorial*, Oxford University Press, New York, 2nd edn, 2006.
28 J. Salvatier, T. Wiecki and C. Fonnesbeck, *PeerJ Comput. Sci.*, 2016, **2**, e55.
29 G. Boniello, C. Blanc, D. Fedorenko, M. Medfai, N. B. Mbarek, M. In, M. Gross, A. Stocco and M. Nobili, *Nat. Mater.*, 2015, **14**, 908–911.
30 N. Sharifi-Mood, I. B. Liu and K. J. Stebe, *Soft Matter*, 2015, **11**, 6768–6779.
31 I. B. Liu, N. Sharifi-mood and K. J. Stebe, *Philos. Trans. R. Soc., A*, 2016, **374**, 20150133.
32 C. Maggi, F. Saglimbeni, M. Dipalo, F. De Angelis and R. Di Leonardo, *Nat. Commun.*, 2015, **6**, 7855.
33 S. Lam, K. P. Velikov and O. D. Velev, *Curr. Opin. Colloid Interface Sci.*, 2014, **19**, 490–500.
34 D. Langevin, *Adv. Colloid Interface Sci.*, 2000, **88**, 209–222.
35 K. Kim, S. Q. Choi, J. A. Zasadzinski and T. M. Squires, *Soft Matter*, 2011, **7**, 7782–7789.
36 S. Sacanna, L. Rossi and A. P. Philipse, *Langmuir*, 2007, **23**, 9974–9982.